

Registration No.

OPSEC#1980



Summary of Gleeble-based, High Temperature Deformation Study on AF9628 Steel

By:

T.M. Lillo, INL

J.A. Simpson, INL

J.K. Walleser, INL

This work was performed for and funded by RDECOM-TARDEC
POC: Victor Burgess, RDECOM-TARDEC

9 January 2019

U.S. Army Tank Automotive Research,
Development, and Engineering Center
Detroit Arsenal
Warren, Michigan 48397-5000

REPORT DOCUMENTATION PAGE

Form Approved
OMB No. 0704-0188

Public reporting burden for this collection of information is estimated to average 1 hour per response, including the time for reviewing instructions, searching existing data sources, gathering and maintaining the data needed, and completing and reviewing this collection of information. Send comments regarding this burden estimate or any other aspect of this collection of information, including suggestions for reducing this burden to Department of Defense, Washington Headquarters Services, Directorate for Information Operations and Reports (0704-0188), 1215 Jefferson Davis Highway, Suite 1204, Arlington, VA 22202-4302. Respondents should be aware that notwithstanding any other provision of law, no person shall be subject to any penalty for failing to comply with a collection of information if it does not display a currently valid OMB control number. **PLEASE DO NOT RETURN YOUR FORM TO THE ABOVE ADDRESS.**

1. REPORT DATE (DD-MM-YYYY)		2. REPORT TYPE	3. DATES COVERED (From - To)		
4. TITLE AND SUBTITLE			5a. CONTRACT NUMBER		
			5b. GRANT NUMBER		
			5c. PROGRAM ELEMENT NUMBER		
6. AUTHOR(S)			5d. PROJECT NUMBER		
			5e. TASK NUMBER		
			5f. WORK UNIT NUMBER		
7. PERFORMING ORGANIZATION NAME(S) AND ADDRESS(ES)			8. PERFORMING ORGANIZATION REPORT NUMBER		
9. SPONSORING / MONITORING AGENCY NAME(S) AND ADDRESS(ES)			10. SPONSOR/MONITOR'S ACRONYM(S)		
			11. SPONSOR/MONITOR'S REPORT NUMBER(S)		
12. DISTRIBUTION / AVAILABILITY STATEMENT					
13. SUPPLEMENTARY NOTES					
14. ABSTRACT					
15. SUBJECT TERMS					
16. SECURITY CLASSIFICATION OF:			17. LIMITATION OF ABSTRACT	18. NUMBER OF PAGES	19a. NAME OF RESPONSIBLE PERSON
a. REPORT	b. ABSTRACT	c. THIS PAGE			19b. TELEPHONE NUMBER (include area code)

Summary of Gleeble-based, High Temperature Deformation Study on AF9628 Steel

T.M. Lillo
J.A.Simpson
J.K. Walleser

December 2018

This work was performed for and funded by RDECOM-TARDEC.

POC: Victor Burgess

RDECOM-TARDEC

6501 E. [11 Mile rd.](#)

RDTA-RTI-GSS-EXTB / MS 263

Warren, MI 48397-5000

victor.w.burguess.civ@mail.mil

victor.w.burguess.civ@mail.smil.mil



The INL is a U.S. Department of Energy National Laboratory
operated by Battelle Energy Alliance

**Distribution A. Approved for public release: Distribution
unlimited. OPSEC#1980**

DISCLAIMER

This information was prepared as an account of work sponsored by an agency of the U.S. Government. Neither the U.S. Government nor any agency thereof, nor any of their employees, makes any warranty, expressed or implied, or assumes any legal liability or responsibility for the accuracy, completeness, or usefulness, of any information, apparatus, product, or process disclosed, or represents that its use would not infringe privately owned rights. References herein to any specific commercial product, process, or service by trade name, trade mark, manufacturer, or otherwise, does not necessarily constitute or imply its endorsement, recommendation, or favoring by the U.S. Government or any agency thereof. The views and opinions of authors expressed herein do not necessarily state or reflect those of the U.S. Government or any agency thereof.

Distribution A. Approved for public release: Distribution unlimited. OPSEC#1980

Summary of Gleeble-based, High Temperature Deformation Study on AF9628 Steel

T.M. Lillo
J.A.Simpson
J.K. Walliser

December 2018

**Idaho National Laboratory
Materials Science and Engineering
Idaho Falls, Idaho 83415**

<http://www.inl.gov>

**Prepared under DOE Idaho Operations Office
Contract DE-AC07-05ID14517**

This work was performed for and funded by RDECOM-TARDEC.
POC: Victor Burgess, RDECOM-TARDEC

Distribution A. Approved for public release: Distribution unlimited. OPSEC#1980

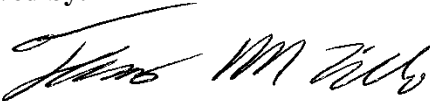
Materials Science and Engineering

**Summary of Gleeble-based, High Temperature Deformation
Study on AF9628 Steel**

**INL/EXT-18-52233
Revision 0**

December 2018

Approved by:



Name: Thomas M. Lillo
Title Senior Materials Engineer/Scientist

12/20/2018
Date

SUMMARY

A study of the high temperature deformation behavior of steel alloy, AF9628, was carried out using the Gleeble 3500 Universal Testing machine. Flow stress data as a function of temperature (900-1175°C) and true strain rate (from 0.1s⁻¹ to 50s⁻¹) for true strains up to 0.5 were collected. This data was used to document the strain sensitivity of this alloy as a function of temperature. It was then used subsequently to develop a deformation processing map which can be used to develop deformation processing schedules, especially rolling reduction schedules, to avoid material failure during thermomechanical processing.

The deformation processing diagram was used to develop potential rolling schedule which were then simulated using the Gleeble 3500. Samples were processed on the Gleeble to simulate 2:1, 3:1 and 8:1 reductions in thickness of a rolling process. The samples were section and studied via optical metallography. Failure of the material was not observed in these samples and it was concluded that the steel could be processed relatively easily between temperatures of 950-1050°C and true strain rates of less than about 10s⁻¹.

CONTENTS

SUMMARY	iv
1. Background.....	1
2. Compression Testing and Development of the Deformation Processing Diagram	1
3. Simulated Rolling Schedules.....	2
4. Considerations for Development of Specific Rolling Schedules for AF9628.....	3
5. References	4
Appendix Simulated Rolling Schedules on Gleeble Samples.....	11

FIGURES

Figure 1. Examples of the specimen before and after compression testing.	5
Figure 2. Example of the flow stress data as a function of temperature and true strain for a true strain rate of (a) 0.1/s and (b) 5/s.	6
Figure 3. Plot showing the strain rate sensitivity as a function of temperature at a true strain of 0.45.	7
Figure 4. The deformation processing map, at a true strain of $\epsilon=0.45$, based on the flow stress data in Table 1. Red boxes denote regions of instability and should be avoided during deformation processing.....	7
Figure 5. Example of multi-pass rolling simulations performed on the Gleeble 3500 using the HydraWedge attachment and the rolling simulation anvils. Each photograph shows the sample after a “hit” (simulating one pass through the rolls) in the programmed, simulated rolling schedule.	8
Figure 6. Metallographic images of the cross section through the specimens subjected to rolling simulations on the Gleeble, (a) Sample 1, (b) Sample 2, (c) Sample 3, (d) Sample 4, (e) Sample 5 and (f) Sample 6.....	9

TABLES

Table 1. Flow Stress Data for AF9628	10
--	----

Summary of Gleeble-based, High Temperature Deformation Study on AF9628 Steel

1. Background

The recently developed steel, AF9628, for high strength and toughness applications may be also applicable to armor applications. To date, this steel has only been forged. However, for armor applications it is desirable to employ rolling reductions of ingots to produce armor plating with thickness ranging up to 2". In an effort to reduce failures associated with a trial-and-error approach for identifying optimal rolling parameters, a study was undertaken to assess the high temperature, strain rate-dependent deformation behavior of small samples. This approach entailed the use of a Gleeble 3500 Universal testing machine to quickly acquire flow stress data as a function of strain rate and temperature on relatively small samples. The variation of flow stress with temperature, strain rate and strain was used to develop a deformation processing diagram following the approach of Prasad [1-3]. This diagram highlights combinations of temperature and strain rate for a given strain that result in microstructural instabilities, such as cracks and adiabatic shear bands, and these combinations should be avoided during deformation processing. In essence, the diagram shows combinations of strain rate and temperature that should result in "sound" material after deformation processing. In this regard, deformation processing diagrams can be used to guide the development of the deformation processing schedule and, at the very least, reducing the number of ingots that need to be sacrificed to develop a suitable deformation processing schedule (in this case, a rolling schedule).

2. Compression Testing and Development of the Deformation Processing Diagram

Compression testing was initially carried out to collect flow stress vs. strain data as a function of temperature and strain rate. Data was collected at temperatures of 900, 1000, 1100 and 1175°C for true strain rates of 0.1, 1.0, 5.0, 10.0 and 50.0 per second. (Generally, typical rolling schedules do not impose true strain rates above about 10/second while forging operations may result in somewhat higher true strain rates.) The temperatures were thought to fall in the stable austenite region of the phase diagram. This steel contains about 0.3 wt% C and based on the iron-carbon phase diagram [4] the ferrite/austenite transformation temperature should be considerably lower than 900°C. The other alloying elements are expected to affect the actual ferrite-to-austenite transformation temperature to some degree. The patent for this steel, US 2016/0369362 A1, refers to a critical austenite temperature of 954°C. However, it is not clear whether this the transformation temperature or, rather, a conservative estimate of a temperature, above which the steel exhibits deformation behavior suitable for forming. In hindsight, the lower temperature of 900°C may have been in the stable ferrite phase field or a mixture of ferrite and austenite.

Compression data was collected on the Gleeble 3500 using the HydraWedge attachment to control deformation strain rates up to 50/second. Right cylinders of AF9628 were obtained from the program sponsor and were 10 mm in diameter and 12 mm tall. GraFoil was placed between the specimen faces and the anvils of the Gleeble to reduce friction at the interface. All specimens

were compressed to a true strain of 0.5 - equivalent to a ~40% reduction in height. (Initially there was a concern that the load capacity of the Gleeble would be exceeded if tests were run to a true strain of 0.7 – equivalent to a 50% reduction in thickness.) Figure 1 shows the test specimen before and after testing. Some barreling is observed, indicating a small but significant amount of friction at the specimen/Gleeble anvil interface.

Figure 2 shows an example of the flow stress versus true strain plots for a true strain rate of 0.1/second, Fig. 2a, and 5/second, Fig. 2b. The high frequency of data collection in Fig. 2a resulted in the thick band of data. Data reduction techniques were used to average the data for use in subsequent analyses. Table 1 summarizes the flow stress as a function of temperature and strain rate at various values of true strain.

Comparing the plots in Figs. 2a and 2b, it is evident that increasing strain rate results in increasing flow stress – the steel exhibits strain rate sensitivity. This behavior is shown more clearly in Fig. 3. A third order polynomial has been applied to the data, however, it should be noted that extrapolation beyond the data to either higher or lower strain rates is not advisable. Using this data and following the method of Prasad, a deformation processing map was developed at true strain of $\epsilon=0.45$, Fig. 4. (Deformation processing maps can also be developed for lower true strain values but the deformation processing map for $\epsilon = 0.45$ represents the most severe case and processing schedules based on this map should be a conservative approach and ensure the best chance of producing “good” material.) The regions in the red boxes represent combinations of strain rate and temperature that result in unstable deformation and should be avoided when developing specific deformation processing schedules. In this study we were unable to investigate the actual mechanism of instability, e.g. cracking, adiabatic shear, etc., associated with each of the red boxes due to the short duration of the project and insufficient funding. As a conservative approach, development of rolling schedules will avoid these regions/conditions to the extent possible.

3. Simulated Rolling Schedules

Some example rolling schedules were developed that were loosely based on the diagram in Fig. 4 and past experience with rolling bainite at INL. The HydraWedge attachment with the anvils for rolling simulations, Fig. 5, were used to test various rolling schedules to verify uniform deformation. The pass-bypass rolling schedules for six samples that were explored are provided in the Appendix. The first sample was subjected to a rolling schedule used previously on a different steel alloy. The remaining samples were subjected to increasingly severe deformation processing conditions – either lower temperatures or higher strain rates. Finally, Sample 6 was subjected to a simulated rolling schedule that consisted of a combination of temperature and strain rate that should have placed it in the red box located on the left-hand side of Fig. 4 in the center (900°C and $\dot{\epsilon}=15/s$). After processing all samples were sectioned and prepared for metallographic analysis. The cross section of each sample is shown in Fig. 6. The samples were etch with Nitol to reveal flow lines. None of the samples exhibited cracking. Only Samples 1 and 6, Figs. 6a and 6f, seem to indicate a shearing type of deformation behavior. The rolling schedule for Sample 1 should have utilized the center of the processing diagram in Fig. 4 – well away from any predicted instability regions. Sample 6, on the other hand, experienced deformation parameters that would have fallen in or at least close to the red box in the center, left-hand side of the processing diagram in Fig. 4. Again, the actual “failure” mechanism associated with this box is not known, nor is it known whether this box actually represents a “failure” as the construction of the box is a purely mathematical prediction. Also, Sample 1 is a 50% reduction in

thickness, meant to simulate reduction of a 4" thick plate to a 2" thick plate. Sample 3 utilizes the same 50% reduction as Sample 1 followed by a re-heat step and a further reduction of another 25%, meant to simulate rolling of a 4" plate to a 2" plate, followed by a re-heat and rolling of the 2" thick plate to a final 1" thick plate. Sample 3 did not show evidence of shearing as observed in Sample 1. It is possible that the simulated "re-heat" step reset the microstructure, allowing it to withstand further reductions. At this time, it is not clear why the microstructure of Sample 1, subjected to a relatively mild reduction schedule, appears to have similar characteristics to Sample 6, which was subjected to an extreme reduction schedule. In any case, the microstructure of the simulated rolling samples indicate this steel is relatively forgiving when it comes to rolling reduction schedules as long as the temperature is between about 1050 and 950°C. (However, it should be noted that the latter passes on Sample 5 were as low as 800°C and it did not show evidence of failure, Fig. 6e, indicating the steel can probably withstand lower temperatures and/or higher strain rates than those predicted by Fig. 4.)

4. Considerations for Development of Specific Rolling Schedules for AF9628

The deformation processing diagram in Fig. 4 shows this steel is actually pretty tolerant of various combinations of strain rates and temperatures. Generally, the potentially "problem" combinations of strain rate and temperature, i.e., the red boxes in Fig. 4, are either difficult to attain in typical rolling schedules (true strain rates $>25/\text{second}$) or appear at lower temperatures, i.e. $<950^\circ\text{C}$, where the steel, presumably, undergoes the austenite-to-ferrite transformation. Therefore, specific rolling schedules should be designed to ensure that *each pass* through the rolls should be performed at no lower than about 950°C (975°C would be a more conservative minimum) and impose a true strain rate somewhere between 0.3s^{-1} and 10s^{-1} . The strain rate on each depends on roller diameter, roll speed (rpm), the reduction in thickness per pass, rolling load/force and the initial thickness of the plate. These parameters are rolling mill equipment-specific and therefore, specific rolling schedules, based on the diagram in Fig. 4, cannot be developed until the rolling mill doing the reductions can be identified and the equipment owner consulted. Once a service provider that can/will perform the rolling reduction is identified, specific rolling schedules will be developed.

As an additional consideration, literature associated with the development of AF9628 suggests a reduction of at least 3:1 to produce a final plate with uniform properties. The as-received slabs are only 4" thick with the final target thickness of some being 2", representing a 2:1 reduction, at best. The other required plate thicknesses will satisfy the 3:1 minimum thickness reduction. Unfortunately, not all the as-received plates are exactly at 4" thick – many are considerably thinner. This almost requires separate rolling schedules for each plate or at least the rolling schedule needs to be evaluated for each plate to ensure the strain rate for each pass remains within the suggested range of 0.3s^{-1} and 10s^{-1} . A final tabulation of the finished dimensions of the machined slabs will be provided to assist the planning and design of the rolling schedule(s).

Finally, the other aspect that will need to be considered is heat loss during the rolling process which will determine when/if the plate needs to be re-heated during the process. Heat loss is a combination of time in contact with the rolls, areal dimension of the plate, the amount of reduction (heating due to plastic deformation) and the amount of time devoted to plate transport between passes (a reversing mill vs. a non-reversing mill). It is likely that re-heating will be necessary especially for plates with a greater total reduction. This is mitigated to some extent by

the need to cut/shear plates during the thickness reduction process to achieve the final desired plate lateral dimensions, especially the thinner plates, e.g., 0.5” and the 0.25” thick plates.

Overall, the most important aspects are to ensure the *plate temperature remains above 950°C* and *to take as large of a reduction per pass without exceeding the mill capacity*. The steel is not particularly sensitive to the strain rate associated with large reductions and the large reduction results in the greatest input of heat due to deformation and minimizes the processing time which reduces time for heat loss.

5. References

- [1] Y.V.R.K. Prasad, “Processing Maps: A Status Report”, JMEPEG, 2003, 12:638-645.
- [2] Y.V.R.K. Prasad and T. Seshacharyulu, “Modelling of hot deformation for microstructural control”, Int. Mater. Rev., 1998, 43:243-258.
- [3] V.V. Balasubrahmanyam and Y.V.R.K. Prasad, “ Hot deformation mechanisms in metastable beta titanium alloy Ti-10V-2Fe-3Al”, Mater. Sci. Tech., 2001, 17:1222-1228.
- [4] K.M. Ralls, T.H. Courtney and J. Wulff, Introduction to Materials Science and Engineering, John Wiley & Sons, New York, 1976, p. 329.



Figure 1. Examples of the specimen before and after compression testing.

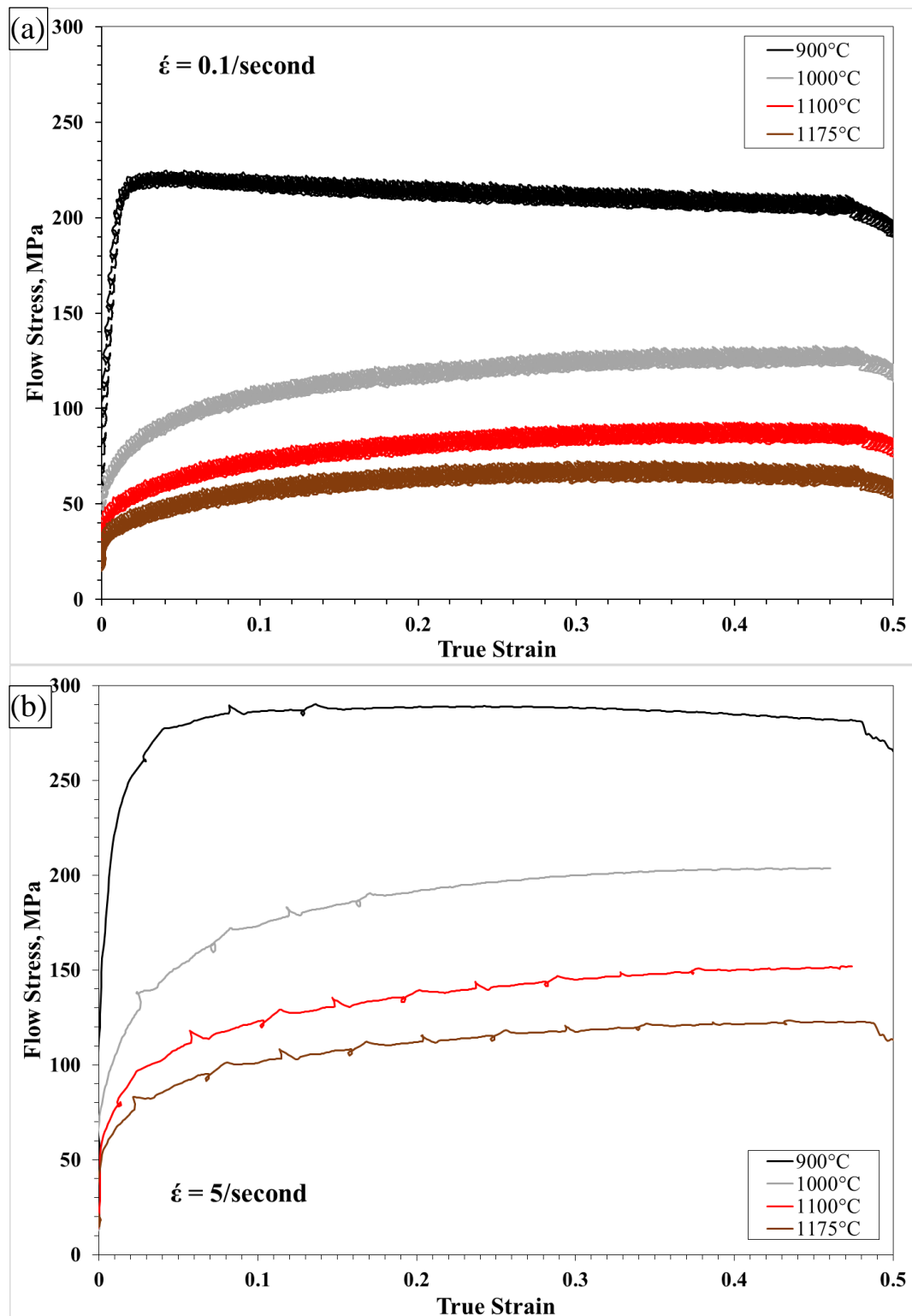


Figure 2. Example of the flow stress data as a function of temperature and true strain for a true strain rate of (a) 0.1/s and (b) 5/s.

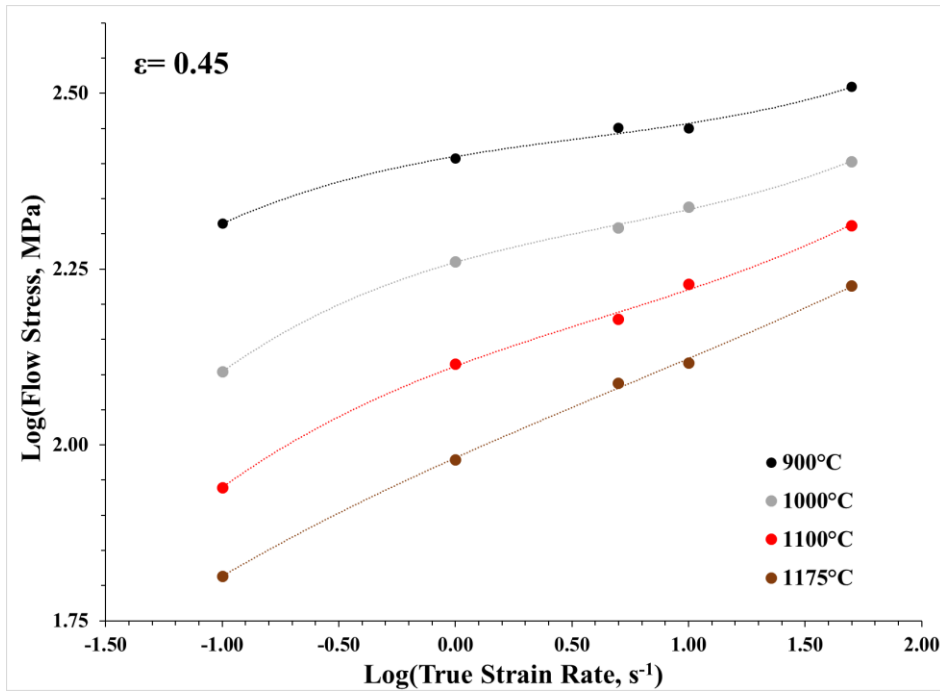


Figure 3. Plot showing the strain rate sensitivity as a function of temperature at a true strain of 0.45.

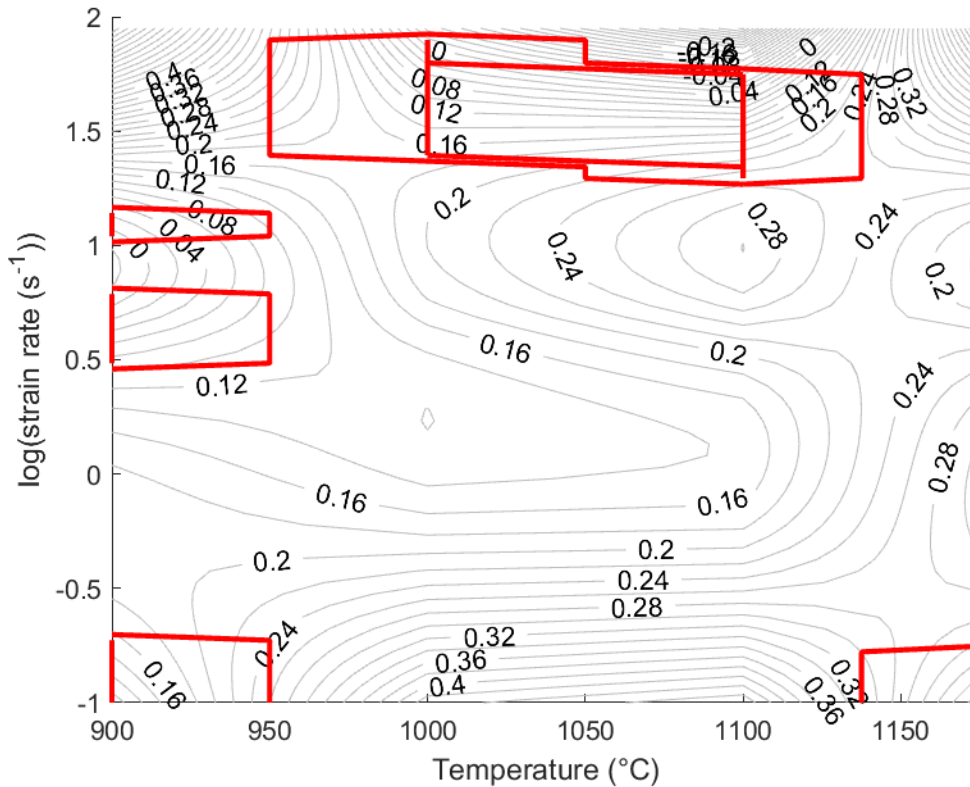


Figure 4. The deformation processing map, at a true strain of $\epsilon=0.45$, based on the flow stress data in Table 1. Red boxes denote regions of instability and should be avoided during deformation processing.

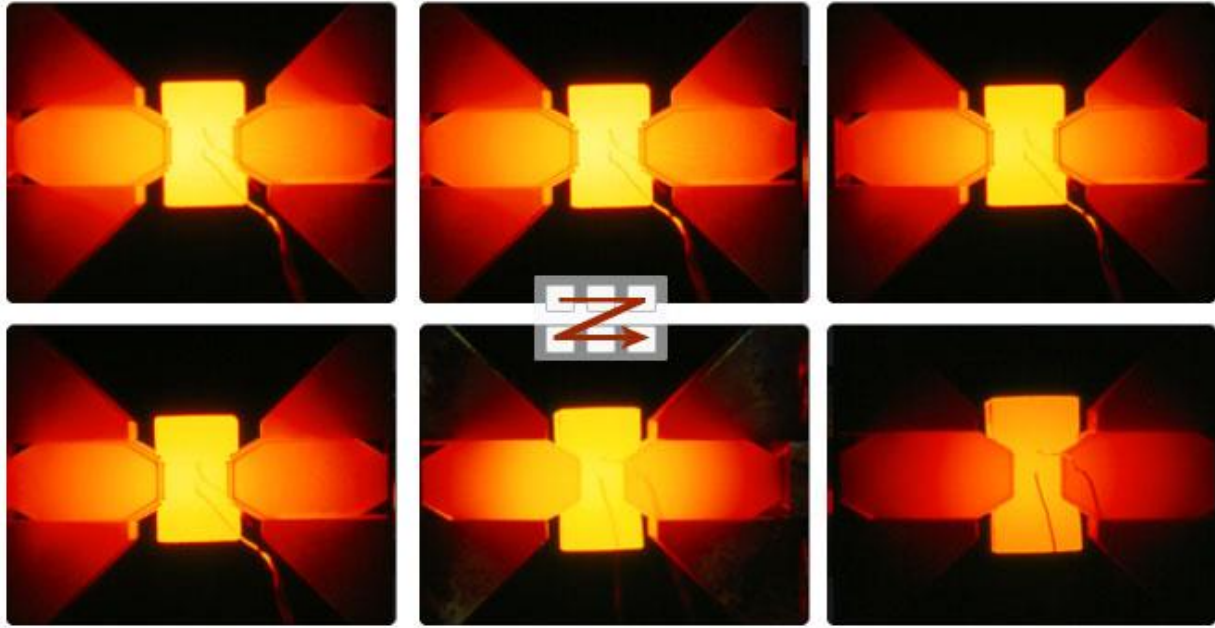


Figure 5. Example of multi-pass rolling simulations performed on the Gleeble 3500 using the HydraWedge attachment and the rolling simulation anvils. Each photograph shows the sample after a “hit” (simulating one pass through the rolls) in the programmed, simulated rolling schedule.

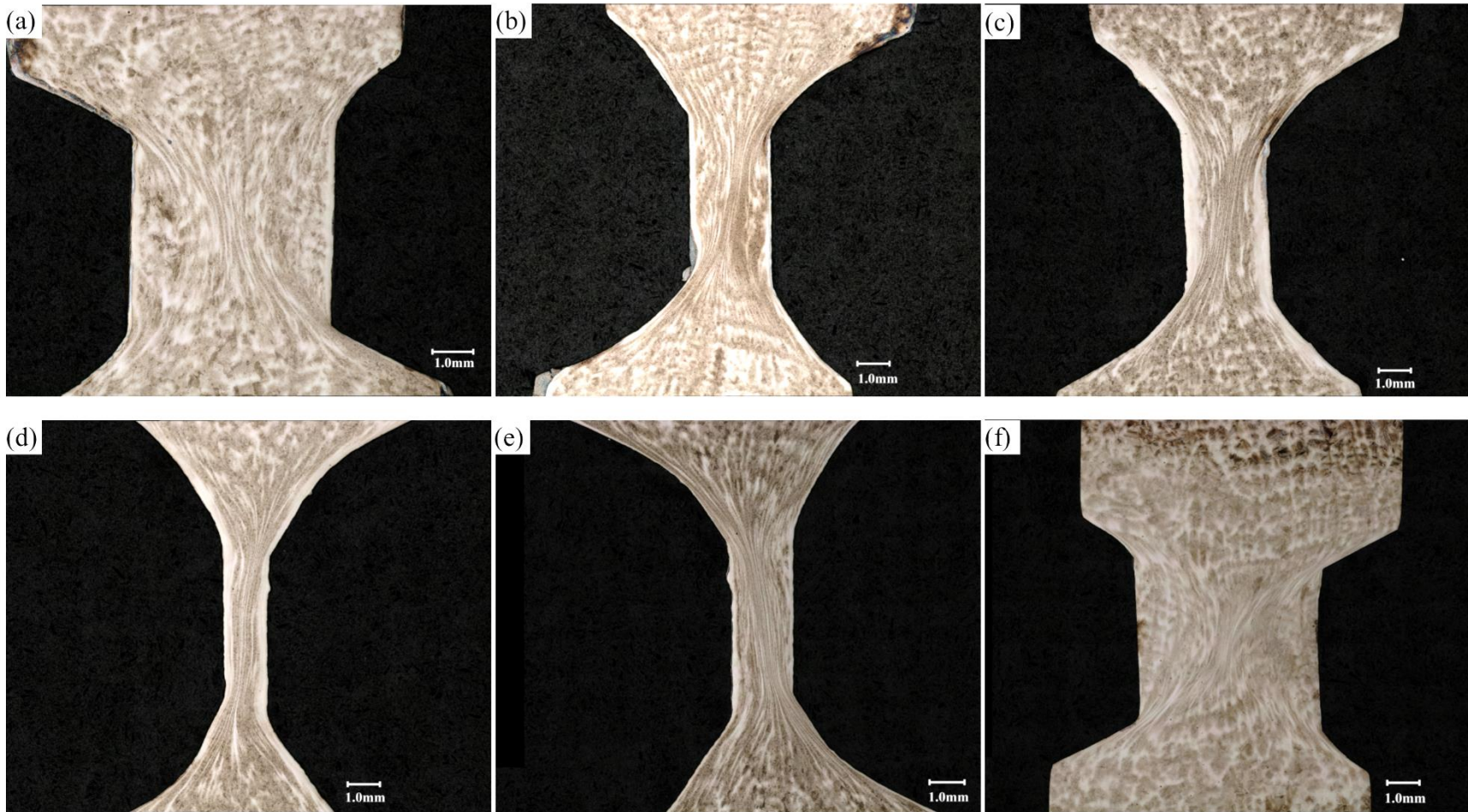


Figure 6. Metallographic images of the cross section through the specimens subjected to rolling simulations on the Gleeble, (a) Sample 1, (b) Sample 2, (c) Sample 3, (d) Sample 4, (e) Sample 5 and (f) Sample 6.

Table 1. Flow Stress Data for AF9628

True Strain	Strain rate, s ⁻¹	Temperature, °C			
		900°C	1000°C	1100°C	1175°C
0.025	0.1	218.2	83.1	55.5	43.2
	1.0	224.3	105.4	78.2	60.3
	5.0	258.6	132.7	96.0	81.0
	10.0	246.4	140.9	102.9	81.8
	50.0	273.4	156.7	123.1	112.4
0.05	0.1	219.9	94.6	63.2	49.3
	1.0	246.9	125.6	90.3	68.0
	5.0	278.6	151.9	108.5	89.8
	10.0	263.8	162.5	121.4	94.7
	50.0	284.2	180.0	142.1	126.9
0.1	0.1	217.6	106.9	72.3	56.8
	1.0	254.0	146.6	102.3	77.7
	5.0	286.2	173.4	122.1	101.3
	10.0	280.7	186.7	139.4	111.1
	50.0	308.7	211.3	161.5	139.1
0.15	0.1	215.3	113.5	77.3	60.9
	1.0	255.6	158.4	109.4	83.6
	5.0	287.6	184.2	132.5	107.4
	10.0	283.6	200.4	147.8	115.1
	50.0	322.1	226.2	179.6	149.7
0.2	0.1	213.7	117.8	81.0	64.0
	1.0	256.6	166.8	114.5	87.5
	5.0	288.5	191.5	138.5	112.9
	10.0	286.3	210.3	155.3	118.6
	50.0	323.1	238.6	188.4	159.5
0.25	0.1	212.3	121.2	83.8	65.8
	1.0	256.9	172.7	119.2	90.2
	5.0	288.7	196.4	141.1	114.9
	10.0	284.9	212.1	162.1	123.1
	50.0	326.5	246.9	192.9	162.2
0.3	0.1	210.8	124.4	85.8	66.6
	1.0	256.9	176.7	123.2	92.0
	5.0	288.2	199.9	145.1	118.1
	10.0	285.8	217.6	163.4	126.9
	50.0	327.7	248.7	197.1	165.2
0.35	0.1	209.3	126.0	86.8	66.9
	1.0	256.5	179.5	126.6	93.4
	5.0	286.7	202.0	147.9	121.1
	10.0	284.5	217.3	168.4	128.8
	50.0	326.8	252.2	202.1	174.2
0.4	0.1	207.7	126.7	87.3	66.2
	1.0	255.9	181.4	128.9	94.0
	5.0	284.7	203.1	150.0	121.5
	10.0	283.3	218.0	168.1	130.3
	50.0	325.6	252.9	204.5	171.2
0.45	0.1	206.5	127.1	86.9	65.1
	1.0	255.6	182.4	130.3	95.4
	5.0	282.4	203.5	150.9	122.5
	10.0	281.9	218.1	169.4	130.8
	50.0	323.1	253.1	205.2	168.3

Appendix

Simulated Rolling Schedules on Gleeble Samples

Sample ID	Rolling pass #	Test Temperature, °C	initial thickness, mm	% reduction	Thickness after pass, mm	Thickness Change, mm	Engg. Strain	True Strain	True Strain Rate, s ⁻¹	Log(strain rate)	Total true strain	Total percent reduction	
1	1	1050	10	3.70	9.63	0.37	-0.037	-0.038	0.80	-0.10	0.038	3.70	
	2	↓	9.63	7.4	8.92	0.71	-0.074	-0.077	1.18	0.07	0.115	10.83	
	3		8.92	8.1	8.20	0.72	-0.081	-0.084	1.28	0.11	0.199	18.05	
	4		8.20	7.8	7.56	0.64	-0.078	-0.081	1.31	0.12	0.280	24.44	
	5		7.56	11.1	6.72	0.84	-0.111	-0.118	1.66	0.22	0.398	32.83	
	6		6.72	8.2	6.17	0.55	-0.082	-0.086	1.49	0.17	0.483	38.34	
	7		6.17	7.2	5.72	0.44	-0.072	-0.075	1.45	0.16	0.558	42.78	
	8		5.72	7	5.32	0.40	-0.070	-0.073	1.48	0.17	0.631	46.78	
	9	950	5.32	5.5	5.03	0.29	-0.055	-0.057	1.35	0.13	0.687	49.71	
2	1	1050	10	3.70	9.63	0.37	-0.037	-0.038	0.80	-0.10	0.04	3.70	
	2	↓	9.63	7.4	8.92	0.71	-0.074	-0.077	1.18	0.07	0.11	10.83	
	3		8.92	8.1	8.20	0.72	-0.081	-0.084	1.28	0.11	0.20	18.05	
	4		8.20	7.8	7.56	0.64	-0.078	-0.081	1.31	0.12	0.28	24.44	
	5		7.56	11.1	6.72	0.84	-0.111	-0.118	1.66	0.22	0.40	32.83	
	6		6.72	8.2	6.17	0.55	-0.082	-0.086	1.49	0.17	0.48	38.34	
	7		6.17	7.2	5.72	0.44	-0.072	-0.075	1.45	0.16	0.56	42.78	
	8		950	5.72	7	5.32	0.40	-0.070	-0.073	1.48	0.17	0.63	46.78
	Anneal 15 minutes at 950°C (simulates re-heat - but should have been 1050°C)												
	9	1050	5.32	5.5	5.03	0.29	-0.055	-0.057	1.35	0.13	0.69	49.71	
	10	↓	5.03	12	4.43	0.60	-0.120	-0.128	2.12	0.33	0.82	55.74	
	11		4.43	9	4.03	0.40	-0.090	-0.094	1.93	0.29	0.91	59.73	
	12		4.03	9	3.66	0.36	-0.090	-0.094	2.02	0.31	1.00	63.35	
	13		3.66	9	3.34	0.33	-0.090	-0.094	2.12	0.33	1.10	66.65	
	14		3.34	12.8	2.91	0.43	-0.128	-0.137	2.71	0.43	1.24	70.92	
15	950		2.91	12	2.56	0.35	-0.120	-0.128	2.79	0.45	1.36	74.41	

Sample ID	Rolling pass #	Test Temperature, °C	initial thickness, mm	% reduction	Thickness after pass, mm	Thickness Change, mm	Engg. Strain	True Strain	True Strain Rate, s ⁻¹	Log(strain rate)	Total true strain	Total percent reduction	
3	1	1050	10	3.70	9.63	0.37	-0.037	-0.038	0.80	-0.10	0.04	3.70	
	2		9.63	7.4	8.92	0.71	-0.074	-0.077	1.18	0.07	0.11	10.83	
	3		8.92	8.1	8.20	0.72	-0.081	-0.084	1.28	0.11	0.20	18.05	
	4		8.20	7.8	7.56	0.64	-0.078	-0.081	1.31	0.12	0.28	24.44	
	5		7.56	11.1	6.72	0.84	-0.111	-0.118	1.66	0.22	0.40	32.83	
	6		6.72	8.2	6.17	0.55	-0.082	-0.086	1.49	0.17	0.48	38.34	
	7		6.17	7.2	5.72	0.44	-0.072	-0.075	1.45	0.16	0.56	42.78	
	8		5.72	7	5.32	0.40	-0.070	-0.073	1.48	0.17	0.63	46.78	
	9	950	5.32	5.5	5.03	0.29	-0.055	-0.057	1.35	0.13	0.69	49.71	
	Anneal 15 minutes at 1050°C (simulates re-heat)												
	10	1050	5.03	12	4.43	0.60	-0.120	-0.128	2.12	0.33	0.82	55.74	
	11		4.43	9	4.03	0.40	-0.090	-0.094	1.93	0.29	0.91	59.73	
	12		4.03	9	3.66	0.36	-0.090	-0.094	2.02	0.31	1.00	63.35	
	13		3.66	9	3.34	0.33	-0.090	-0.094	2.12	0.33	1.10	66.65	
	14		3.34	12.8	2.91	0.43	-0.128	-0.137	2.71	0.43	1.24	70.92	
15	950	2.91	12	2.56	0.35	-0.120	-0.128	2.79	0.45	1.36	74.41		

Sample ID	Rolling pass #	Test Temperature, °C	initial thickness, mm	% reduction	Thickness after pass, mm	Thickness Change, mm	Engg. Strain	True Strain	True Strain Rate, s ⁻¹	Log(strain rate)	Total true strain	Total percent reduction	
4	1	1050	10	20.00	8.00	2.00	-0.200	-0.223	2.04	0.31	0.22	20.00	
	2	↓	8.00	15	6.80	1.20	-0.150	-0.163	1.92	0.28	0.39	32.00	
	3		6.80	10	6.12	0.68	-0.100	-0.105	1.65	0.22	0.49	38.80	
	4		6.12	10	5.51	0.61	-0.100	-0.105	1.74	0.24	0.60	44.92	
	5		950	5.51	9	5.01	0.50	-0.090	-0.094	1.73	0.24	0.69	49.88
	Anneal 5 minutes at 1050°C												
	10	1050	5.01	20	4.01	1.00	-0.200	-0.223	2.12	0.33	0.91	59.90	
	11	↓	4.01	15	3.41	0.60	-0.150	-0.163	1.93	0.29	1.08	65.92	
	12		3.41	15	2.90	0.51	-0.150	-0.163	2.02	0.31	1.24	71.03	
	13		950	2.90	12	2.55	0.35	-0.120	-0.128	2.12	0.33	1.37	74.51
	Anneal 5 minute at 1050°C												
	16	1050	2.55	15	2.17	0.38	-0.150	-0.163	2.54	0.40	1.53	78.33	
	17	↓	2.17	15	1.84	0.33	-0.150	-0.163	2.82	0.45	1.69	81.58	
	18		1.84	15	1.57	0.28	-0.150	-0.163	2.80	0.45	1.85	84.34	
	19		1.57	15	1.33	0.23	-0.150	-0.163	3.11	0.49	2.02	86.69	
	20		950	1.33	7	1.24	0.09	-0.070	-0.073	3.10	0.49	2.09	87.62
	Sample ID	Rolling pass #	Test Temperature, °C	initial thickness, mm	reduction	Thickness after pass, mm	Thickness Change, mm	Engg. Strain	True Strain	True Strain Rate, s ⁻¹	Log(strain rate)	Total true strain	Total percent reduction
	5	1	1050	10	20.00	8.00	2.00	-0.200	-0.223	2.04	0.31	0.22	20.00
		2	↓	8.00	15	6.80	1.20	-0.150	-0.163	1.92	0.28	0.39	32.00
		3		6.80	10	6.12	0.68	-0.100	-0.105	1.65	0.22	0.49	38.80
4		6.12		10	5.51	0.61	-0.100	-0.105	1.74	0.24	0.60	44.92	
5		5.51		9	5.01	0.50	-0.090	-0.094	1.73	0.24	0.69	49.88	
6		5.01		20	4.01	1.00	-0.200	-0.223	2.12	0.33	0.91	59.90	
7		4.01		15	3.41	0.60	-0.150	-0.163	1.93	0.29	1.08	65.92	
8		3.41		15	2.90	0.51	-0.150	-0.163	2.02	0.31	1.24	71.03	
9		2.90		12	2.55	0.35	-0.120	-0.128	2.12	0.33	1.37	74.51	
10		2.55		15	2.17	0.38	-0.150	-0.163	2.54	0.40	1.53	78.33	
11		2.17		15	1.84	0.33	-0.150	-0.163	2.82	0.45	1.69	81.58	
12		1.84		15	1.57	0.28	-0.150	-0.163	2.80	0.45	1.85	84.34	
13		1.57		15	1.33	0.23	-0.150	-0.163	3.11	0.49	2.02	86.69	
14		800		1.33	7	1.24	0.09	-0.070	-0.073	3.10	0.49	2.09	87.62

Sample ID	Rolling pass #	Test Temperature, °C	initial thickness, mm	reduction	Thickness after pass, mm	Thickness Change, mm	Engg. Strain	True Strain	True Strain Rate, s ⁻¹	Log(strain rate)	Total true strain	Total percent reduction
6	1	900	10	30.00	7.00	3.00	-0.300	-0.357	15.00	1.18	0.36	30.00
	2		7.00	15	5.95	1.05	-0.150	-0.163	10.00	1.00	0.52	40.50
	3		5.95	10	5.36	0.60	-0.100	-0.105	1.65	0.22	0.62	46.45
	4	900	5.36	7	4.98	0.37	-0.070	-0.073	1.74	0.24	0.70	50.20